

Modeling the light curve of Type II_n-P SN 2005cl with red supergiant progenitors featuring pre-SN outbursts

Chunhui Li,¹★Viktoria Morozova^{1,2}†

¹Department of Physics, The Pennsylvania State University, University Park, PA 16802-6300, USA

²Institute for Gravitation and the Cosmos, The Pennsylvania State University, University Park, PA 16802-6300, USA

3 January 2022

ABSTRACT

All Type II_n supernovae (SNe II_n) show narrow hydrogen emission lines in their spectra. Apart from this common feature, they demonstrate very broad diversity in brightness, duration, and morphology of their light curves, which indicates that they likely come from a variety of progenitor systems and explosion channels. A particular subset of SNe II_n, the so called SNe II_n-P, exhibit ~100 days plateau phases that are very similar to the ones of the ordinary hydrogen-rich SNe (SNe II). In the past, SNe II_n-P were explained by the models of sub-energetic electron capture explosions surrounded by dense extended winds. In this work, we attempt to explain this class of SNe with standard red supergiant (RSG) progenitors that experience outbursts several month before the final explosion. The outburst energies that show the best agreement between our models and the data (5×10^{46} erg) fall at the low range of the outburst energies that have been observed for SNe II_n (between few times 10^{46} erg and 10^{49} erg). Instead, the inferred explosion energy of SN 2005cl is relatively high ($1 - 2 \times 10^{51}$ erg) compared to the explosion energies of the ordinary SNe II. Our models provide alternative explanation of SNe II_n-P to the previously proposed scenarios.

Key words: supernovae: general – supernovae: individual: SN 2005cl

1 INTRODUCTION

Hydrogen-rich supernovae (SNe) that exhibit narrow Balmer emission lines in their spectra are commonly distinguished as a separate subclass of SNe, the so called Type II_n (Schlegel 1990). SNe II_n are often brighter than regular hydrogen-rich SNe and exhibit more extended light curves (Kiewe et al. 2012; Nyholm et al. 2020). It has long been understood that the narrow lines in their spectra originate from the interaction of shocked ejecta with the slow and dense material located ahead of the shock (Chugai 1991; Chugai & Danziger 1994; Chugai 2001; Chugai et al. 2004). Moreover, it has been recognized that almost any astrophysical explosion, such as core-collapse or thermonuclear SN, may appear as a SN II_n if surrounded by a sufficient amount of the circumstellar material (CSM) (Smith 2017). Indeed, the broad diversity of light curves that can be classified as Type II_n suggests that they may originate from very different progenitors (see, for example, Taddia et al. 2013; Fox et al. 2013; Haberman et al. 2014; de la Rosa et al. 2016).

A variety of mechanisms could lead to the formation of this CSM, ranging from enhanced pre-SN winds to the binary interactions (Moriya 2014; Moriya et al. 2014a; Andrews et al. 2017; Kurfürst et al. 2020). One of the most promising scenarios is that this material forms as a result of a violent mass eruption due to the core nuclear burning in the last years before the SN explosion (Quataert & Shiode 2012; Shiode & Quataert 2014; Dessart et al. 2016; Fuller 2017; Das & Ray 2017; Leung & Fuller 2020; Takei et al. 2021; Wu & Fuller 2021). This idea is supported by numerous observations of SN pre-

cursors, outbursts that happen months to years prior to SNe II_n (Ofek et al. 2013; Mauerhan et al. 2013a; Fraser et al. 2013; Margutti et al. 2014; Tartaglia et al. 2016; Elias-Rosa et al. 2016; Ofek et al. 2016; Thöne et al. 2017; Nyholm et al. 2017; Pastorello et al. 2018; Reguitti et al. 2019). Some of the largest collections of SN II_n precursors can be found in Ofek et al. (2014) and Strotjohann et al. (2021).

Contrary to SNe II_n, the ordinary hydrogen-rich plateau SNe (SNe II) were thought to originate from red supergiant (RSG) progenitors surrounded by regular low-density stellar winds. Only in recent years the early observations of SNe II started to indicate that their progenitors may also be surrounded by the dense CSM (Gal-Yam et al. 2014; Smith et al. 2015; Khazov et al. 2016; Yaron et al. 2017; Hosseinzadeh et al. 2018; Nakaoka et al. 2018; Bullivant et al. 2018). This is supported by hydrodynamical simulations of their light curves, which show significantly better agreement with the observational data when the dense CSM is added to the models (Nagy & Vinkó 2016; Morozova et al. 2017, 2018; Paxton et al. 2018; Moriya et al. 2018; Förster et al. 2018). In addition, the analysis of late-time nuclear burning in RSG cores shows that they are capable of generating the outbursts with sufficient energy (Fuller 2017). The fact that no precursors prior to regular SNe II have been detected yet (Kochanek et al. 2017; Johnson et al. 2018; O’Neill et al. 2019) may indicate that they are weaker and shorter living than the SN II_n precursors.

That said, there potentially exists a group of SNe that originates from common RSG progenitors, spans across the II and II_n classes, and can be described by a continuously varying characteristics of a pre-SN outburst (energy or timing). Indeed, the observed progenitors of some SNe II_n have moderate masses of $10 M_{\odot}$ which are typical of RSGs (Prieto et al. 2008; Szczygiel et al. 2012). Moreover, Mauerhan et al. (2013b) distinguishes a subclass of SNe (SNe II_n-P) that exhibit

★ Contact e-mail: cpl5430@psu.edu

† Contact e-mail: vzg5138@psu.edu

narrow lines in their spectra, yet demonstrate features that are typical of regular plateau SNe (see also [Smith 2017](#)).

In this work, we use radiation hydrodynamics simulations to probe the idea that SNe IIn-P may come from regular RSG progenitors that experience eruptive outbursts before their explosions. We construct a grid of theoretical light curves that differ by the outburst energy, the final SN energy, and the time interval between the outburst and the SN explosion. With this grid, we look for the best fitting model of SN 2005cl ([Kiewe et al. 2012](#)), which is a member of IIn-P class. We confirm that this SN could originate from a RSG progenitor and give a rough estimate of the outburst and explosion parameters for the class.

The rest of this paper is organized as follows. In Section 2, we describe our numerical setup. Section 3 contains our main results, and Section 4 is devoted to the conclusions and discussion.

2 NUMERICAL SETUP

We carry out our research using the publicly available code SNEC ([Morozova et al. 2015](#)). SNEC solves the Lagrangian hydrodynamics equations coupled with radiation transport in the flux-limited diffusion approximation. This code is well suited for modeling bolometric light curves of SNe II starting from few days after the shock breakout until the end of the plateau phase. We work with two RSG stellar evolution models at the onset of core-collapse, both taken from the KEPLER set by [Sukhbold et al. \(2016\)](#). At zero-age main sequence (ZAMS) these models had masses $10 M_{\odot}$ and $15 M_{\odot}$. The final mass of the $10 M_{\odot}$ RSG before the core collapse is $9.7 M_{\odot}$, and its radius is $513 R_{\odot}$. The final mass of the $15 M_{\odot}$ RSG before the core collapse is $12.6 M_{\odot}$, and its radius is $841 R_{\odot}$.

In the first stage of our modeling, we inject a certain amount of energy, E_{inj} , at the base of the hydrogen envelope of the RSG. This step is meant to simulate a weak outburst caused by a convectively driven wave during vigorous late-stage nuclear burning in the RSG core ([Fuller 2017](#)). To inject the energy into the $10 M_{\odot}$ model, we first excise its core down to the density 0.89 g cm^{-3} ($2.13 M_{\odot}$ in terms of excised inner mass). In the $15 M_{\odot}$ model, we excise the core down to the density 1.13 g cm^{-3} ($4.31 M_{\odot}$ in terms of excised inner mass)¹. We utilize the thermal bomb mechanism and inject the energy in the zone with density $0.52 \times 10^{-4} \text{ g cm}^{-3}$, at the interface between He core and H envelope. The injected energy, E_{inj} , takes the values 0.5, 1.0, 2.0, 3.0 and $4.0 \times 10^{47} \text{ erg}$.

The weak shock wave caused by the energy injection takes about 100 days to propagate out to the surface of the RSG and preheat its envelope. Once it reaches the surface, it causes ejection of the outermost material and expansion of the star. The amount of the ejected material depends on the energy E_{inj} . We follow the evolution of the model for up to ~ 2 years after the energy injection and collect the snapshots of its profile at different times, t_{inj} , for the subsequent explosion with typical SN energies. That is, t_{inj} in our models is the time between the energy injection at the base of the H envelope and the SN explosion.

¹ The amount of mass that we excise at this stage does not carry any physical meaning, but it is determined solely by the balance of factors influencing the feasibility of our numerical simulations. On the one hand, we want the inner boundary of our model to be deeper than the interface between He core and H envelope where we inject the energy. On the other hand, not excising the core leads to slow simulations and numerical problems at the center, since SNEC is not a stellar evolution code and it is not meant to support RSG cores for an extended period of time.

In the second stage of our modeling, we process the collected profiles in SNEC using regular core-collapse SN setup ([Morozova et al. 2015](#)). Before exploding the models as regular SNe, we attach back their core parts that were excised earlier, assuming that they have not been affected by the weak energy injection. Then, we deposit the explosion energy into the innermost zones of the models, now excising only $1.4 M_{\odot}$ of material, which is meant to form a stable neutron star remnant. We use four values for the final energy², $E_{\text{fin}} = 0.5, 1.0, 1.5, \text{ and } 2.0 \times 10^{51} \text{ erg}$. As a result, we obtain a coarse three-dimensional grid of SN light curves differing by E_{inj} , t_{inj} , and E_{fin} . Parsing through this grid we look for the light curve that fits best the data of SN 2005cl by minimizing χ^2 between the data and the theoretical light curves. A very similar approach has been adopted in our earlier works, [Morozova et al. \(2020\)](#) and [Tinyanont et al. \(2021\)](#) (see also [Grasberg & Nadezhin 1986, 1991](#)).

One more parameter that has to be chosen in SNEC simulations is the mass of radioactive ^{56}Ni responsible for the radioactive tail of the light curve. In SNe IIn the ^{56}Ni mass is not constrained as well as in regular SNe II, and we did not find the estimate for the ^{56}Ni mass of SN 2005cl in the literature. For this reason, in our simulation we used an average ^{56}Ni mass typical for SNe II, $M_{\text{Ni}} = 0.05 M_{\odot}$ (in SNe II, the ^{56}Ni masses range between $\sim 0.001 M_{\odot}$ and $\sim 0.1 M_{\odot}$, somewhat clustering around $0.05 M_{\odot}$; see [Valenti et al. 2016](#)). When comparing the resulting light curves to the data (in the next section), we see that this value slightly overestimates the observed brightness of the tail, but not by much. In addition, SNEC is less accurate in modeling the radioactive tails of SN light curves compared to their plateau parts, because the black body approximation is no longer suitable after the end of the plateau. For now, we adopt this value of M_{Ni} assuming that it does not strongly affect the deduction of parameters that are of our main interest here (E_{inj} , t_{inj} , and E_{fin}).

3 RESULTS

Figs. 1-3 show the light curves obtained from our models versus the observed light curve of SN 2005cl in V-band. In all three figures, the red bold lines represent the best fitting light curves for the corresponding RSG progenitor ($10 M_{\odot}$ or $15 M_{\odot}$), while the other curves show how the light curve changes when we vary one of the model parameters (E_{inj} , E_{fin} , or t_{inj}).

In Fig. 1, we plot the light curves of $10 M_{\odot}$ (top panel) and $15 M_{\odot}$ (bottom panel) RSG models with the final energies $E_{\text{fin}} = 1.5 \times 10^{51} \text{ erg}$ and $2.0 \times 10^{51} \text{ erg}$, respectively. Different light curves correspond to the different outburst energies E_{inj} . The plot demonstrates that the outburst energy has even greater influence on the level and duration of the plateau than it has on the early light curve. Stronger outbursts correspond to markedly brighter and longer plateau phases in both progenitor models. The data show the agreement with relatively modest outburst energies of $5.0 \times 10^{46} \text{ erg}$ for the $10 M_{\odot}$ progenitor and $10.0 \times 10^{46} \text{ erg}$ for the $15 M_{\odot}$ progenitor. These values are on the lower end of the range of outburst energies measured by [Strotjohann et al. \(2021\)](#) (between 3 and $1000 \times 10^{46} \text{ erg}$).

Almost all light curves in Fig. 1 show very sharp transition between the plateau phase and the ^{56}Ni tail which is typical of SNe IIn-P ([Smith 2017](#)). Note that we used only one value for the ^{56}Ni mass, which is close to the average value for SNe II, whereas the observations of SNe IIn-P suggest low ^{56}Ni yields. Lower values of

² In SNEC, $E_{\text{fin}} = E_{\text{init}} + E_{\text{bomb}}$ represents the final energy of the model, where E_{init} is its total initial energy, and E_{bomb} is the energy deposited in the thermal bomb.

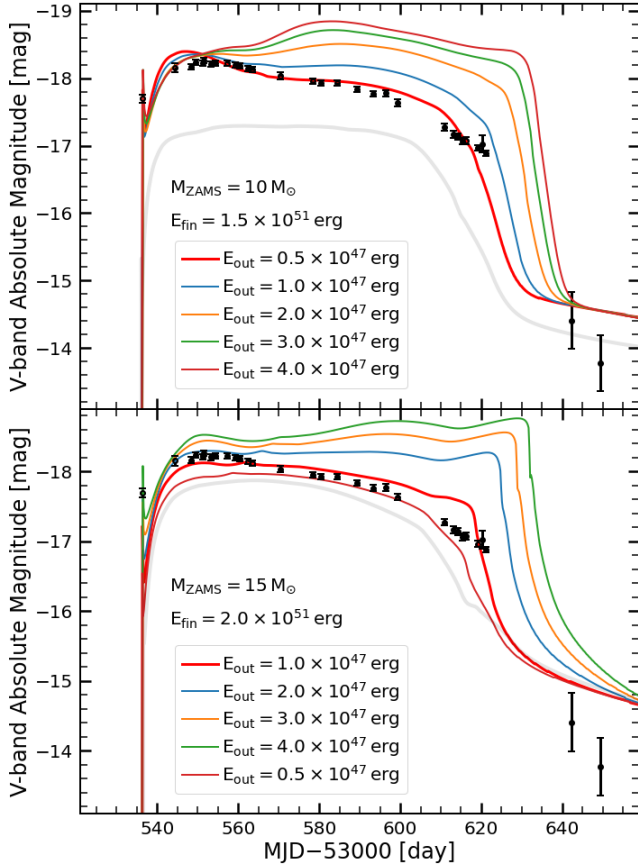


Figure 1. The V-band light curves of the models preheated with different energies E_{inj} , compared to the data of SN 2005cl. The top panel shows the $10 M_{\odot}$ progenitor, and the bottom panel shows the $15 M_{\odot}$ progenitor. All curves shown in the top panel correspond to same final energy $E_{\text{fin}} = 1.5 \times 10^{51}$ erg and time $t_{\text{inj}} = 258$ days. All curves from the bottom panel have the final energy $E_{\text{fin}} = 2.0 \times 10^{51}$ erg and time $t_{\text{inj}} = 258$ days. The light curves of bare RSG models with the corresponding explosion energies are shown in gray. The red curve in each panel is the best fitting light curve for that progenitor model.

^{56}Ni mass would make the transition even sharper and lead to a better agreement between the data and our models during the tail phase. On the other hand, it would make the end of the plateau dimmer and shorter, which could favor the models with slightly larger outburst energies.

The gray curves in both panels show the light curves obtained from the bare RSG models with the same explosion energies. The plateau brightness of these light curves is insufficient to fit the data, however, the larger explosion energies would make the plateau even shorter. In addition, not preheated RSG models would have more difficulties reproducing the early (~ 20 days post explosion) peak and subsequent decline of the observed light curve. This indicates that simulating pre-SN outbursts plays a crucial role in fitting SNe II-P light curves by RSG progenitors.

In Fig. 2, we plot the light curves of both models for different values of final energies E_{fin} , while keeping E_{inj} constant. The plots demonstrate a well-known trend, where an increase in the explosion energy leads to a brighter but shorter plateau (Litvinova & Nadezhin 1983; Kasen & Woosley 2009; Bersten et al. 2011). The best fitting

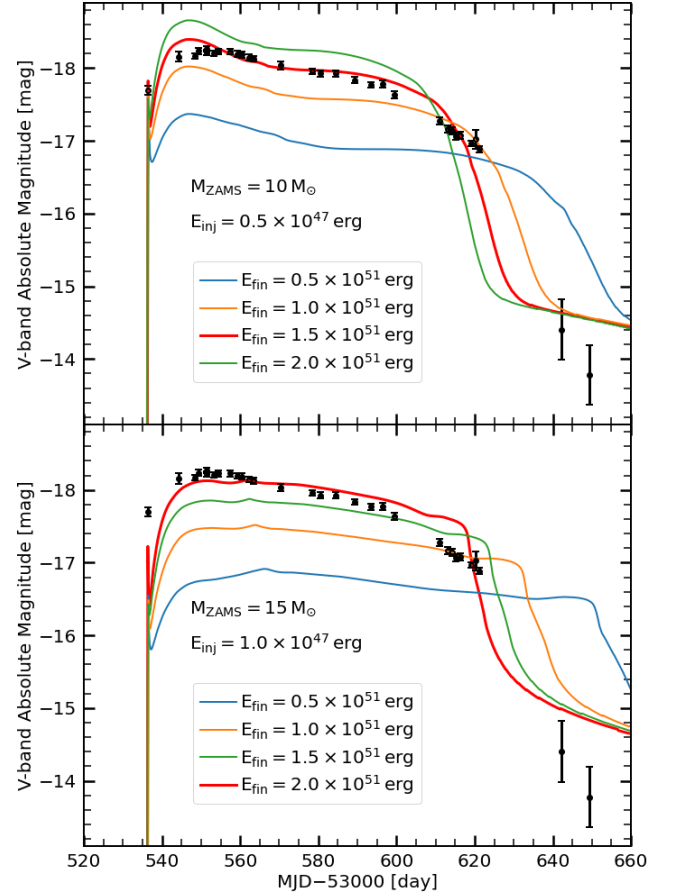


Figure 2. The V-band light curves of the models exploded with different final energies E_{fin} , compared to the data of SN 2005cl. The top panel shows the $10 M_{\odot}$ progenitor, and the bottom panel shows the $15 M_{\odot}$ progenitor. All curves shown in the top panel correspond to the same outburst energy $E_{\text{out}} = 0.5 \times 10^{47}$ erg and time $t_{\text{inj}} = 258$ days. All curves from the bottom panel have the same $E_{\text{out}} = 1.0 \times 10^{47}$ erg and time $t_{\text{inj}} = 258$ days. The red curve in each panel is the best fitting light curve for that progenitor model.

models have $E_{\text{fin}} = 1.5 \times 10^{51}$ erg for the $10 M_{\odot}$ progenitor and $E_{\text{fin}} = 2.0 \times 10^{51}$ erg for the $15 M_{\odot}$ progenitor.

Fig. 3 shows the light curves obtained from the models with same E_{inj} and E_{fin} , but different time intervals between the weak outburst and the SN explosion, t_{inj} . Lighter colors correspond to shorter t_{inj} , and vice versa. For the small values of t_{inj} , the SN explosion happens while the outer layers of the star are still expanding after being preheated, which leads to the brighter light curves, especially during the first 30 – 40 days past explosion. However, if t_{inj} is sufficiently large, some of the material ejected in the weak outburst starts to fall back down onto the star. This is clearly seen in Fig. 3 for the $10 M_{\odot}$ progenitor (top panel), where the shape of the early light curves becomes different for the models with large t_{inj} . The same is not seen for the $15 M_{\odot}$ progenitor because of the larger outburst energy E_{inj} .

The best fitting models for both $10 M_{\odot}$ and $15 M_{\odot}$ progenitors have $t_{\text{inj}} = 258$ days. This agrees with the results of Strotjohann et al. (2021), where the outbursts were seen anywhere between few tens of days to ~ 700 days prior to the SN explosions.

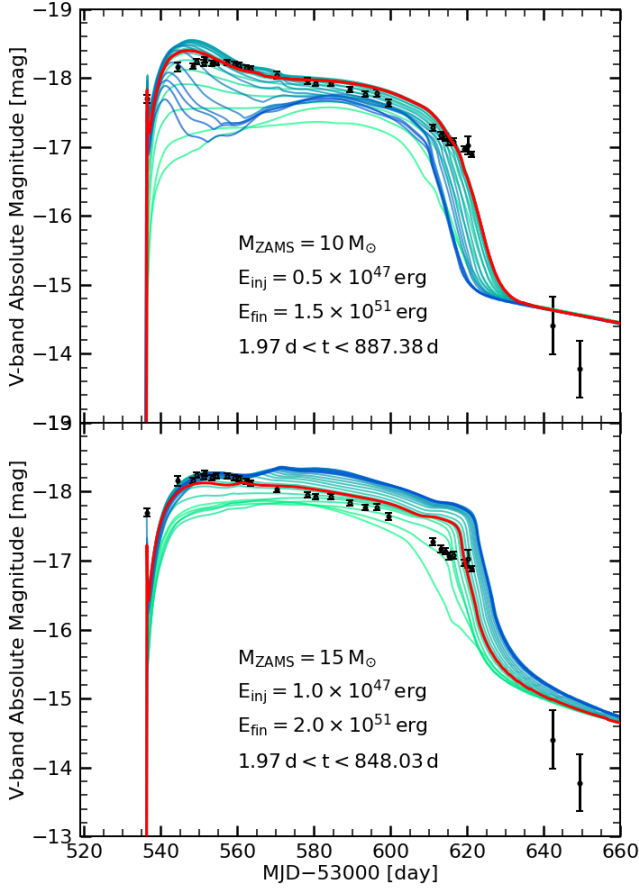


Figure 3. The V-band light curves of the $10 M_{\odot}$ and $15 M_{\odot}$ models with different time intervals t_{inj} between the weak outburst and the SN explosion.

4 SUMMARY AND DISCUSSION

We have simulated a grid of theoretical light curves from two RSG models preheated by relatively small amount of energy injected at the base of their hydrogen envelopes few days to a few years prior to their explosions as core-collapse SNe. These models are meant to represent SNe preceded by weak outbursts. Varying the outburst energies, the explosion energies, and the time interval between the outburst and the explosion, we found a set of parameters that matches the light curve of SN 2005cl. In our picture, this SN could originate from a relatively low mass, $10 M_{\odot}$ RSG progenitor that experienced a 5×10^{46} erg outburst 258 days before it exploded with final energy 1.5×10^{51} erg.

SN 2005cl belongs to the class of SNe IIn-P (Mauerhan et al. 2013b; Smith 2017), whose members have persistent narrow hydrogen lines in their spectra yet show the characteristics of ordinary SNe II such as a ~ 100 days plateau steeply transitioning into a radioactive tail. Among other SNe that belong to the same class are 1994W, 2011ht, and 2009kn. These SNe have similar plateau lengths between 100 and 125 days, and they vary in plateau brightness by ~ 2 magnitudes, with SN 2005cl being the brightest of the four (see Mauerhan et al. 2013b). We speculate that the fits to the other SNe from this group may be found among the models with similar parameters to the one of SN 2005cl. Accurate modeling would require larger number of theoretical light curves than presented here and more precise estimates of the radioactive ^{56}Ni mass. However, already with the models shown here we can see that the outburst plays a very impor-

tant role in extending the plateau to the observed length. A bare RSG model exploded with energy needed to reproduce the bright plateau would produce a much shorter light curve lasting only 60 – 80 days (see Fig. 2).

If the circumstellar material surrounding the SNe before their explosion forms in an eruptive outburst, it would be interesting to compare the amounts of the outburst energy needed to explain the observations of SNe IIn versus regular SNe II. There are relatively few models of SNe II with pre-SN outbursts, but some of the published ones indicate that the outburst energy of $\sim 5 \times 10^{46}$ erg is sufficient to bring the models in good agreement with observational data (Morozova et al. 2020; Tinyanont et al. 2021). The models presented here indicate that the amount of energy needed to explain SNe IIn-P is roughly the same. It is possible to explain the injection of this energy into the base of the hydrogen envelope by the late-time nuclear burning processes happening in the RSG cores (Fuller 2017).

Similarity of the energies needed for the outbursts in SNe IIn-P and regular SNe II returns us back to the question of why there is still no ordinary SN II with a documented pre-SN outburst. In our opinion, the reason lies in the weakness of the outburst light curve for that amount of energy. Looking at the pre-SN data of SNe with similar outburst energies from Strotjohann et al. (2021), we see that those outbursts are very hard to recognize with a naked eye, because they are short lived and embedded in noisy data (see, for example, SN 2019bxq with the outburst energy 3×10^{46} erg released ~ 350 and ~ 180 days before the SN, or SN 2018eru with the outburst energy 4×10^{46} erg released ~ 200 and ~ 65 days before the SN). Extracting those outbursts from the data required delicate techniques such as forced photometry and light curve binning (Strotjohann et al. 2021).

On the other hand, if SNe IIn-P and regular SNe II experience similar pre-SN outbursts, why do we not see narrow lines in the spectra of the latter? A possible answer to this question lies in the analysis performed by Strotjohann et al. (2021) of the impact of pre-SN outbursts on the SN spectra. Specifically, the authors showed that almost none of the outbursts detected in the last years before the explosion could be responsible for the formation of narrow lines in the spectra of the subsequent SNe. This is because the radius of material accountable for the narrow lines (as estimated from the spectra) is significantly larger than the radius to which the outburst material could have possibly expanded by that time (as estimated from the timing of the outbursts using a broad range of ejecta velocities). Therefore, it was concluded that earlier episodes of mass eruption that happened years prior to the observed outbursts would be needed to explain the narrow lines seen in the spectra (see also Moriya et al. 2014a). Almost all transients described in Strotjohann et al. (2021) were pre-selected to be of type IIn (except one superluminous SN II, and one SN Ia), because this type was previously associated with the pre-SN activity. However, the outbursts that happen within a year of the explosion do not necessarily cause the long lasting narrow lines, and may instead cause only the so called flash ionization seen in the very early (hours to days) spectra of many SNe II (Khazov et al. 2016; Yaron et al. 2017; Lin et al. 2021). It would be very interesting to look at a sample of regular well-observed SNe II with sufficient pre-SN data, and check whether or not there are low energy outbursts in the data.

In view of our models, the main parameter that distinguishes SNe IIn-P from ordinary SNe II is the final energy of the explosion. To achieve high plateau brightness seen in SNe IIn one needs the energies of the order of a few times 10^{51} erg. On the other hand, the final energies of regular SNe II lie in the range between 0.2 and 1×10^{51} erg clustering around 0.5×10^{51} erg (see, for example, Pumo et al. 2017; Morozova et al. 2018). Interestingly, some of the previous models

suggested that SNe IIn-P originate from low energy ($\sim 10^{50}$ erg) electron capture explosions (see, for example [Moriya et al. 2014b](#); [Smith 2017](#)), which would be consistent with low ^{56}Ni yield seen in these SNe. In our models, lower explosion energies would lead to the dimmer and longer plateau phases incompatible with observations, whereas larger outbursts energies would also increase the length of the plateau. More accurate investigation of this topic will be the subject of our future study.

ACKNOWLEDGEMENTS

This research was supported by the undergraduate summer research program (REU) of the Physics Department of the Pennsylvania State University.

DATA AVAILABILITY

The data underlying this article will be shared on reasonable request to the corresponding author.

REFERENCES

- Andrews J. E., Smith N., McCully C., Fox O. D., Valenti S., Howell D. A., 2017, *MNRAS*, **471**, 4047
- Bersten M. C., Benvenuto O., Hamuy M., 2011, *ApJ*, **729**, 61
- Bullivant C., et al., 2018, *MNRAS*, **476**, 1497
- Chugai N. N., 1991, *MNRAS*, **250**, 513
- Chugai N. N., 2001, *MNRAS*, **326**, 1448
- Chugai N. N., Danziger I. J., 1994, *MNRAS*, **268**, 173
- Chugai N. N., et al., 2004, *MNRAS*, **352**, 1213
- Das S., Ray A., 2017, *ApJ*, **851**, 138
- Dessart L., Hillier D. J., Audit E., Livne E., Waldman R., 2016, *MNRAS*, **458**, 2094
- Elias-Rosa N., et al., 2016, *MNRAS*, **463**, 3894
- Förster F., et al., 2018, *Nature Astronomy*, **2**, 808
- Fox O. D., Filippenko A. V., Skrutskie M. F., Silverman J. M., Ganeshalingam M., Cenko S. B., Clubb K. I., 2013, *AJ*, **146**, 2
- Fraser M., et al., 2013, *ApJ*, **779**, L8
- Fuller J., 2017, *Monthly Notices of the Royal Astronomical Society*, **470**, 1642
- Gal-Yam A., et al., 2014, *Nature*, **509**, 471
- Grasberg E. K., Nadezhin D. K., 1986, *Soviet Astronomy Letters*, **12**, 68
- Grasberg E. K., Nadezhin D. K., 1991, *Soviet Ast.*, **35**, 42
- Habergham S. M., Anderson J. P., James P. A., Lyman J. D., 2014, *MNRAS*, **441**, 2230
- Hosseinzadeh G., et al., 2018, *ApJ*, **861**, 63
- Johnson S. A., Kochanek C. S., Adams S. M., 2018, *MNRAS*, **480**, 1696
- Kasen D., Woosley S. E., 2009, *ApJ*, **703**, 2205
- Khazov D., et al., 2016, *ApJ*, **818**, 3
- Kiewe M., et al., 2012, *ApJ*, **744**, 10
- Kochanek C. S., et al., 2017, *MNRAS*, **467**, 3347
- Kurfürst P., Pejcha O., Krtićka J., 2020, *A&A*, **642**, A214
- Leung S.-C., Fuller J., 2020, *The Astrophysical Journal*, **900**, 99
- Lin H., et al., 2021, *MNRAS*, **505**, 4890
- Litvinova I. I., Nadezhin D. K., 1983, *Ap&SS*, **89**, 89
- Margutti R., et al., 2014, *ApJ*, **780**, 21
- Mauerhan J. C., et al., 2013a, *MNRAS*, **430**, 1801
- Mauerhan J. C., et al., 2013b, *MNRAS*, **431**, 2599
- Moriya T. J., 2014, *A&A*, **564**, A83
- Moriya T. J., Maeda K., Taddia F., Sollerman J., Blinnikov S. I., Sorokina E. I., 2014a, *MNRAS*, **439**, 2917
- Moriya T. J., Tominaga N., Langer N., Nomoto K., Blinnikov S. I., Sorokina E. I., 2014b, *A&A*, **569**, A57
- Moriya T. J., Förster F., Yoon S.-C., Gräfenner G., Blinnikov S. I., 2018, *MNRAS*,
- Morozova V., Piro A. L., Renzo M., Ott C. D., Clausen D., Couch S. M., Ellis J., Roberts L. F., 2015, *ApJ*, **814**, 63
- Morozova V., Piro A. L., Valenti S., 2017, *ApJ*, **838**, 28
- Morozova V., Piro A. L., Valenti S., 2018, *ApJ*, **858**, 15
- Morozova V., Piro A. L., Fuller J., Van Dyk S. D., 2020, *The Astrophysical Journal Letters*, **891**, L32
- Nagy A. P., Vinkó J., 2016, *A&A*, **589**, A53
- Nakaoka T., et al., 2018, *ApJ*, **859**, 78
- Nyholm A., et al., 2017, *A&A*, **605**, A6
- Nyholm A., et al., 2020, *A&A*, **637**, A73
- O’Neill D., et al., 2019, *A&A*, **622**, L1
- Ofek E. O., et al., 2013, *Nature*, **494**, 65
- Ofek E. O., et al., 2014, *ApJ*, **789**, 104
- Ofek E. O., et al., 2016, *ApJ*, **824**, 6
- Pastorello A., et al., 2018, *MNRAS*, **474**, 197
- Paxton B., et al., 2018, *ApJS*, **234**, 34
- Prieto J. L., et al., 2008, *ApJ*, **681**, L9
- Pumo M. L., Zampieri L., Spiro S., Pastorello A., Benetti S., Cappellaro E., Manicò G., Turatto M., 2017, *MNRAS*, **464**, 3013
- Quataert E., Shiode J., 2012, *MNRAS*, **423**, L92
- Reguitti A., et al., 2019, *MNRAS*, **482**, 2750
- Schlegel E. M., 1990, *MNRAS*, **244**, 269
- Shiode J. H., Quataert E., 2014, *ApJ*, **780**, 96
- Smith N., 2017, *Interacting Supernovae: Types IIn and Ibn*, p. 403, doi:10.1007/978-3-319-21846-5_38
- Smith N., et al., 2015, *MNRAS*, **449**, 1876
- Strotjohann N. L., et al., 2021, *ApJ*, **907**, 99
- Sukhbold T., Ertl T., Woosley S. E., Brown J. M., Janka H. T., 2016, *ApJ*, **821**, 38
- Szczygieł D. M., Kochanek C. S., Dai X., 2012, *ApJ*, **760**, 20
- Taddia F., et al., 2013, *A&A*, **555**, A10
- Takei Y., Tsuna D., Kuriyama N., Ko T., Shigeyama T., 2021, arXiv e-prints, p. arXiv:2109.05871
- Tartaglia L., et al., 2016, *MNRAS*, **459**, 1039
- Thöne C. C., et al., 2017, *A&A*, **599**, A129
- Tinyanont S., et al., 2021, *MNRAS*,
- Valenti S., et al., 2016, *MNRAS*, **459**, 3939
- Wu S., Fuller J., 2021, *The Astrophysical Journal*, **906**, 3
- Yaron O., et al., 2017, *Nature Physics*, **13**, 510
- de la Rosa J., Roming P., Pritchard T., Fryer C., 2016, *ApJ*, **820**, 74

This paper has been typeset from a \LaTeX file prepared by the author.